Environ. Sci. Technol. **1998**, *32,* 2749−2754

Heavy Metal Ion Adsorbents Formed by the Grafting of a Thiol Functionality to Mesoporous Silica Molecular Sieves: Factors Affecting Hg(II) Uptake

LOUIS MERCIER AND
THOMAS J. PINNAVAIA*
Department of Chemistry and Center for Fundamental Materials Research, Michigan State University, East Lansing, Michigan 48824

A new approach to heavy metal ion adsorbents based on the covalent grafting of 3-mercaptopropylsilyl groups to the framework pore walls of mesoporous silica molecular sieves has been investigated with regard to hydroxyl group densities, channel dimensions, and morphologies. Two types of silicas were examined, namely, MCM-41 with an initially anionic silicate framework and HMS with an electrically neutral framework. The MCM-41 derivative was obtained through electrostatic $S^+X^-I^+$ assembly, where S^+ was a quaternary ammonium ion surfactant, X^- was a halide, and I^+ was the silica precursor derived from tetraethyl orthosilicate (TEOS) in acidic solution. HMS silicas were assembled by a S°I° pathway using alkylamines as surfactants (S°) and TEOS as the neutral silica source (I°). Prior to thiol functionalization of the mesostructures by a one-step grafting procedure, S^+ was removed from MCM-41 by calcination, whereas for HMS, S° was removed by solvent extraction. The grafting process was much more effective for the functionalization of HMS than for MCM-41 owing to a higher surface concentration of surface hydroxyl groups. Consequently, the functionalized HMS derivative was able to bind quantitatively more Hg(II) ions from aqueous solution compared to MCM-41. The Hg(II) adsorption capacities for HMS were interpreted in terms of the size and accessibility of the framework pore structure.

Introduction

Heavy metals, particularly mercury and lead, are important environmental pollutants, threatening the health of human populations and natural ecosystems alike. Removal of these species from the environment is thus a major focus of waste treatment and cleanup efforts. Several adsorptive compounds can capture metal ions from solution, including activated charcoal (*1*), zeolites (*2, 3*), and clays (*4, 5*). An inherent disadvantage of these materials is their low loading capacities and relatively small metal ion binding constants. To circumvent these limitations, promising heavy metal sorbents have been prepared by the coupling of chelating ligands (e.g., thiol, amine, or crown ether functions) to support matrixes consisting of inorganic oxides (e.g., silica, alumina, or clay) (*6*−*22*) or organic polymers [e.g., polystyrene, cellulose, or poly(methyl methacrylate)] (*23*−*28*). Such functionalized materials have relatively high metal ion loading capacities and strong binding affinities for selected metal ions. This exceptional performance can be attributed to the presence of the surface-bound ligands, which can be specifically tuned to accommodate the selective adsorption of targeted metal ions. These functionalized oxides and polymers have been used in the preconcentration of metal ions for the assaying of multicomponent solutions (*28*) and for the removal of toxic species from wastewater streams, in particular, radionuclides (*22*). Although superior in performance to conventional ion exchangers, functionalized matrixes remain relatively inefficient because only a fraction of the immobilized ligands are accessible for metal complexation.

The recent discovery of mesoporous metal oxide molecular sieves by Mobil researchers has given rise to new prospects for adsorbent and catalyst design (*29*). Recently, we reported the preparation of highly effective heavy metal ion adsorbents by grafting thiol moieties to the pore channel walls of mesoporous silica molecular sieves (*30*). Our functionalized absorbent, denoted MP-HMS, exhibited Hg(II) binding sufficiently efficient to achieve federal drinking water standards, along with an unprecedented loading capacity of 310 mg/g (1.5 mmol/g). The most interesting property, perhaps, was the ability of the absorbent to bind mercury ions quantitatively to each ligand site in the material, a result attributable to the uniform and large framework pore structure (2.7 nm) of the absorbent.

Concurrent with our report on thiol-funtionalized HMS silica, Feng and co-workers (*31*) reported an analogous heavy metal ion adsorbent based on the mercaptopropylsilyl functionalization of a calcined form of mesoporous MCM-41 silica. Although their grafting approach was analogous to that reported previously for the functionaliztion of MCM-41 (*32, 33*), a much higher concentration of immobilized ligand was achieved through the use of a larger pore framework (5.5 nm) and a functionalization process that involved repeated surface hydrolysis and silylation cycles. The mercury loading (505 mg/g) was even higher than that observed for functionalized HMS.

Hexagonal MCM-41 silica is normally prepared by hydrothermal S^+I^- assembly, where S^+ is an onium ion surfactant and I^- an anionic inorganic precursor (silicate) (*29*). The removal of the surfactant template from this compound by calcination results in a silica derivative with ordered pore channels of well-defined diameters (2−10 nm) and very high surface areas (500−1200 m^2/g). An alternative method of obtaining MCM-41 involves a counterion-mediated $S^+X^-I^+$ assembly pathway in acidic aqueous solutions at room temperature (*34*). This latter process also affords a hexagonal silica framework upon calcination, but with some disorder in the packing of the channels (*34*). However, for both of these electrostatically assembled materials, the calcination process typically used to remove the surfactant from the framework depletes the surfaces of hydroxyl groups for organosilane functionalization, which is undesirable from the standpoint forming heavy metal traps. Although the electrostatically bound surfactant in MCM-41 can be removed by ion exchange (*37*), the exchange process requires strong acid conditions, so there is little or no advantage of ion exchange over surface rehydroxylation after calcination.

Electrically neutral framework analogues of mesoporous silica molecular sieves may be synthesized using alkylamines (*36*) and nonionic surfactants (*37*) as structure directors. These materials are denoted as HMS and MSU-X, repectively. Unlike MCM-41, HMS and MSU-X materials typically consist

* Author to whom correspondence should be addressed.

S0013-936X(97)00622-6 CCC: $15.00
Published on Web 08/12/1998

of disordered assemblies of wormlike channels. Moreover, because of the absence of a framework charge, the surfactant molecules can be removed from the channels by solvent extraction and recycled. This facile removal of the surfactant optimizes the number of surface hydroxyl groups that are available on the pore walls for a organosilane functionalization.

In this paper, we examine the Hg-binding properties of thiol-functionalized mesoporous molecular sieves with different pore dimensions and channel morphologies. We also compare the effectiveness of a *one-step* silylation process for the functionalization of mesoporous frameworks prepared by electrostatic and electrically neutral assembly pathways. The adsorbents include an MCM-41 prepared by $S^+X^-I^+$ assembly, and two HMS silica compositions of differing pore diameter prepared by S°I° assembly. The grafting moiety was mercaptopropyltrimethoxysilane, $(CH_3O)_3SiCH_2CH_2CH_2$-SH, which has a strong binding affinity for mercury. The efficiency toward Hg(II) binding is shown for the first time to depend critically on the pore size of the functionalized mesoporous molecular sieve. Also, HMS is shown to be more effectively functionalized with siloxane thiol groups in a one-step silylation process compared to calcined MCM-41, owing primarily to the higher surface density of framework hydroxyl groups. The results reported here should be useful in evaluating these materials for environmental cleanup and heavy metal ion recovery.

Materials and Methods

Mesostructure Syntheses. HMS silica molecular sieves were synthesized by a S°I° assembly process using neutral amines surfactants as framework structure directors and subsequently removing the neutral surfactant by solvent extraction (*35*). HMS-C12 silica was obtained by first dissolving 1.35 g of dodecylamine in 10 mL of ethanol, adding water to obtain a fine emulsion, then adding tetraethyl orthosilicate (TEOS) under vigorous stirring. 1,3,5,-Trimethylbenzene (TMB) was added and the reaction mixture was stirred vigorously for 20 h at room temperature. The molar ratio of reagents was 1.0 TEOS:0.23 amine:0.23 TMB:160 water. The precipitated product was filtered, washed with water, and allowed to dry at room temperature for 24 h. The powder was then washed free of the surfactant by Soxhlet extraction over ethanol for 72 h. An analogous smaller pore mesostructure, denoted HMS-C8, was prepared from octylamine following the same experimental protocol, with the exception that TMB was omitted from the synthesis mixture and no ethanol was added to the reaction medium.

MCM-41 was prepared by $S^+X^-I^+$ assembly at room temperature in acidic media using a quaternary ammonium ion surfactant and TMB as a cosurfactant and subsequently removing the surfactant by calcination. The reagent molar ratio was 1 TEOS:1 HCl:0.2 octylamine:1 TMB:150 water. The product was filtered, air-dried and calcined at 650 °C for 4 h in order to remove the surfactant from the framework channels.

Mesostructure Functionalization. A 1 g quantity of each surfactant-free mesostructure was dried under vacuum at 110 °C and refluxed in 25 mL of dry toluene containing 1.0 g of 3-mercaptopropyltrimethoxysilane for 24 h. The dried materials were then recovered by filtration and washed with toluene followed by ethanol. Any residual organosilane was removed by Soxhlet extraction over ethanol for 24 h. The mercaptopropylsilyl-functionalized mesostructures are henceforth denoted as MP-MCM-41, MP-HMS-C12, and MP-HMS-C8.

Materials Characterization. The parent mesostructures (HMS-C12, HMS-C8, and MCM-41) were structurally characterized by powder X-ray diffraction, N_2 surface area analysis, and ^{29}Si MAS NMR spectroscopy. The mercaptopropylsilyl-functionalized analogues were characterized using the same techniques, as well as by elemental analysis.

Powder X-ray diffraction (XRD) patterns for HMS and MP-HMS were recorded on a Rigaku rotaflex diffractometer using Ni-filtered Cu Kα radiation. Proton-decoupled ^{29}Si MAS NMR spectra were recorded on a Varian VRX 400 MHz spectrometer at 79.5 MHz using 7 mm zirconia rotors, a sample spinning frequency of 4 kHz, and a pulse delay of 870 s. Nitrogen adsorption isotherms were measured at 77 K on a Coulter Omnisorp 360CX Sorptometer using standard continuous adsorption procedures. The samples were heated overnight at 110 °C and 10^{-6} Torr prior to measurement. C, H, N, and S analyses were performed in duplicate by the Microanalysis Laboratory at the University of Illinois at Urbana-Champaign. Particle size analyses for MCM-41 and HMS-C12 were performed on a Micromeritics SediGraph 5100 particle size analyzer.

Mercury Adsorption Studies. Ten milligram quantities of mesostructured adsorbent were stirred for 18 h with 50 mL of mercury(II) nitrate solutions of known concentration. Adsorption points were obtained by allowing a suspension of 10 mg of MP-HMS in 50 mL of Hg(II) solution (0−35 ppm) to equilibrate at room temperature for 18 h and measuring the Hg(II) uptake by difference. The Hg(II) concentrations of the supernatant liquids were measured before and after treatment by colorimetric assays using diphenylthiocarbazone as an indicator (*38*). Blank experiments on nonfunctionalized MCM-41 and HMS silicas were carried out using 50 mg samples and 50 mL of 4.0 ppm Hg(II) solutions. Hg analyses were also performed on the mercury-loaded adsorbents to confirm Hg uptake by the materials.

Results and Discussion

Adsorbent Characterization. Figure 1 compares the XRD patterns of MCM-41 and HMS prior to and following functionalization with mercaptopropyltrimethoxysilane. The XRD pattern of MCM-41, which contains a dominant d_{100} reflection and a broad d_{110} reflection at higher diffraction angle, is consistent with disordered hexagonal channel packing (*34*). The XRD lines of HMS-C12 and HMS-C8 are substantially broader than those of MCM-41. The broad XRD lines, together with TEM images of HMS silicas, have been previously interpreted (*39*) in terms of wormhole channel motifs.

Organosilane grafting to the mesostructures causes a significant decrease in XRD intensities. The decrease in peak intensities is indicative of contrast matching between the silica framework and the grafted mercaptopropylsilyl groups. Contrast matching in MCM-41 and related mesostructures has been observed previously upon filling the framework pores with organic guests (*40*, *41*). The smaller contrast-matching effect in the case of MP-MCM-41 probably results from the comparatively lower amount of mercaptopropylsilyl groups occupying the framework pore structure (see below).

The N_2 adsorption isotherms of the unfunctionalized mesostructures shown in Figure 2 contain linear to step-shaped uptakes at partial pressures between 0.1 and 0.6. These features are indicative of the presence of framework mesopores. The BET surface areas (854−1264 m^2/g) were within the range expected for mesostructured materials. The Horvath−Kawazoe pore size distributions (Figure 2, insets) further verified the presence of mesoporous channels in the range 1.9−3.6 nm. Upon grafting mercaptopropylsiloxane groups to the framework walls, we observe a significant decrease in the surface area, pore volume, and pore diameter for each sample as a result of the ligating thiol moieties present in the framework channels. Nonetheless, significant surface areas and porosities were retained in all the mesostructures after mercaptopropylsilyl functionalization of the

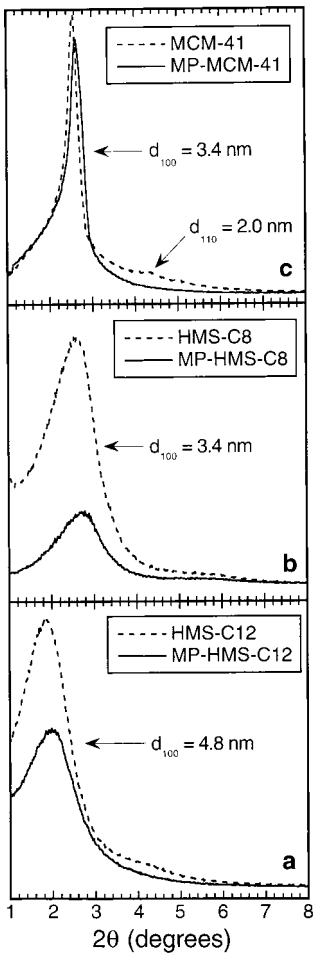

FIGURE 1. Powder X-ray diffraction patterns for mesoporous molecular sieves. (Dashed lines) (a) HMS-C12, (b) HMS-C8, and (c) MCM-41 and their mercaptopropylsilyl-functionalized derivatives (solid lines) (a) MP-HMS-C12, (b) MP-HMS-C8, and (c) MP-MCM-41.

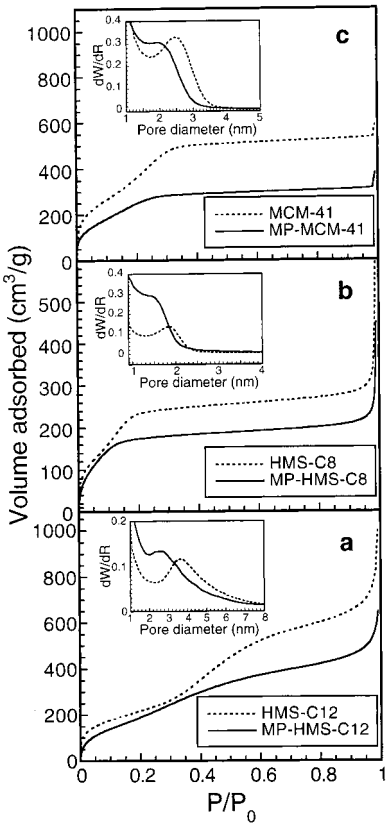

FIGURE 2. Nitrogen adsorption isotherms for mesoporous molecular sieves. (Dashed lines) (a) HMS-C12, (b) HMS-C8, and (c) MCM-41 and their mercaptopropylsilyl-functionalized derivatives (solid lines) (a) MP-HMS-C12, (b) MP-HMS-C8, and (c) MP-MCM-41. P/P_0 is the relative pressure, where P is the equilibrium pressure of the adsorbate and P_0 its saturation pressure at the adsorbent temperature; the volume adsorbed is at STP. (Inset) Pore size distributions based on the Horvath−Kawazoe model [dW/dR is the derivative of the normalized adsorbate (nitrogen) volume adsorbed with respect to the pore diameter of the adsorbent].

pore walls. The surface properties of the MP-functionalized adsorbents and their parent mesostructures are summarized in Table 1.

The C, H, N, and S analyses of the adsorbents were used to determine the quantity of mercaptopropylsilyl moieties grafted to the framework channels (MP-HMS-C12, 9.19 wt % C, 2.15 wt % H, and 4.82 wt % S; MP-HMS-C8, 7.71 wt % C, 1.96 wt % H, and 2.90 wt % S; MP-MCM-41, 3.96 wt % C, 1.25 wt % H, and 1.79 wt % S). The absence of detectable levels of nitrogen in the materials demonstrated the effectiveness of the ethanol extraction process in removing the amine surfactants from the HMS silicas. The amounts of SH groups present in the adsorbents are shown in Table 1. On the basis of these loadings and the BET surface areas of the unfunctionalized mesostructures, we calculated the SH group densities on the pore walls of the adsorbents (see Table 1).

The low mercaptopropylsilyl group density in MP-MCM-41 (0.28 SH/nm^2) can be attributed to the relative scarcity of surface hydroxyl groups on the pore walls. Significant dehydroxylation is expected upon the removal of the surfactant at high calcination temperature (650 °C), thus limiting the amount of organosilane that may be grafted in the channels. For MP-HMS-C12 and MP-HMS-C8, however, the much higher mercaptopropylsilyl group density observed (0.49 and 1.2 SH/nm^2) can be attributed to the more abundant hydroxyl groups present in the parent mesostructures. In this latter case, low-temperature solvent extraction techniques were effective in removing the surfactants from the framework pores, resulting in hydroxylated surfaces that are much more reactive than MCM-41 toward organosilane grafting. The relatively low level of grafted mercaptopropylsilyl groups in MP-HMS-C8 compared to MP-HMS-C12 can be explained by steric factors in the smaller pores of HMS-C8 which prevent the grafting of a significant percentage of the framework hydroxyls.

^{29}Si MAS NMR spectra of the unfunctionalized mesostructures (see Figure 3) were obtained in order to estimate the Q^3 to Q^4 ratios and the fraction of framework silicon sites that have been silylated. In both HMS-C8 and HMS-C12, two signals were observed near −103 and −114 ppm, corresponding to the Q^3 silanol sites [$(SiO)_3SiOH$] and Q^4 framework silica sites [$(SiO)_4Si$], respectively (*32*). Grafting of the mercaptopropylsilyl moieties to these mesostructures causes the relative Q^3/Q^4 signal intensities to decrease significantly. In addition, a new signal appears at about −55 ppm, which we assigned to the silicon of the grafted mercaptopropylsilyl group. These results indicate that the Si−OH sites lining the pore walls of the materials undergo condensation reaction with the organosilane coupling agent, forming a covalent linkage to the silica framework. Because the Q^3 signal in the MCM-41 spectrum was not well resolved (appearing as a very broad shoulder on the −114 ppm signal), an accurate assessment of the silanol grafting was not possible in this material.

On the basis of both ^{29}Si NMR data and elemental analyses results (C, H, and S), we obtained empirical formulas for the

TABLE 1. Summary of the Physical Characteristics for Mesoporous Molecular Sieves and Their Mercaptopropyl-Functionalized Analogs

material	BET surface area (m^2/g)	pore diameter (nm)[a]	SH content (mmol/g)[b]	SH groups per nm^2	pore volume (cm^3/g)[c]	chemical formula
HMS-C12	854	3.6	0	0	0.85	$(SiO_2)_{0.56}(SiO_{2.5}H)_{0.44}$
MP-HMS-C12	722	2.7	1.5	1.2	0.55	$(SiO_2)_{0.83}(SiO_{2.5}H)_{0.17}$ $[SiO_{1.15}(OCH_3)_{0.7}(CH_2)_3SH]_{0.12}$
HMS-C8	1200	1.9	0	0	0.37	$(SiO_2)_{0.53}(SiO_{2.5}H)_{0.47}$
MP-HMS-C8	640	1.5	0.90	0.49	0.27	$(SiO_2)_{0.73}(SiO_{2.5}H)_{0.27}$ $[SiO_{1.5}(CH_2)_3SH]_{0.066}$
MCM-41	1264	2.5	0	0	0.77	$(SiO_2)_{1-x}(SiO_{2.5}H)_x$, $x < 0.3$
MP-MCM-41	1061	2.0	0.57	0.28	0.44	$(SiO_2)[SiO_{0.5}(OCH_3)_2(CH_2)_3SH]_{0.037}$

[a] See Figure 2 for pore size distributions. [b] Millimoles of S per gram of MP-functionalized adsorbent. [c] Expressed as a volume of liquid N_2.

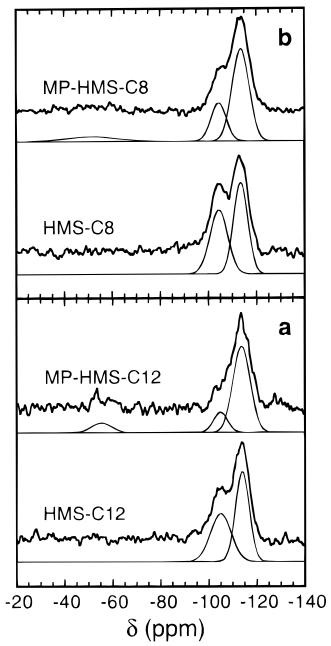

FIGURE 3. ^{29}Si MAS NMR spectra for mesoporous molecular sieves and their mercaptopropylsilyl-functionalized derivatives: (a) HMS-C12 (bottom) and MP-HMS-C12 (top), (b) HMS-C8 (bottom) and MP-HMS-C8 (top). The dotted lines represent deconvoluted signals fitted using Gaussian line shape analysis.

HMS mesostructures and their functionalized analogues. In these structures, the Q^4 sites are represented by the formula unit (SiO_2) and the Q^3 silanol sites by the unit ($SiO_{2.5}H$). The grafting of 3-mercaptopropyltrimethoxysilane [$Si(OCH_3)_3$-$(CH_2)_3SH$] to the mesostructures may involve the condensation of one, two or three Si-OCH_3 groups to an equivalent number of surface Si-OH groups. A general reaction formula for the grafting reaction can be written as

$$(SiO_2)_{1-x}(SiO_{2.5}H)_x + SiX_3(CH_2)_3SH \rightarrow (SiO_2)_{1-x+yz}(SiO_{2.5}H)_{x-yz}[SiO_{z/2}X_{3-z}(CH_2)_3SH]_y + yzHX\ (X = OCH_3) \quad (1)$$

where x represents the molar fraction of framework silicon atoms initially present as Q^3 (Si-OH) sites, y is the mercaptopropyl group stoichiometric factor, and z is the average number of Si-O bonds formed per grafted organosilane molecule.

Table 1 shows the chemical formulas of the functionalized mesostructures deduced on the basis of eq 1. For HMS-C12 and HMS-C8, 44−47% of the framework silicon atoms are initially hydroxylated. Calcined MCM-41 prepared by the $S^+X^-I^+$ assembly pathway exhibits relatively broad ^{29}Si resonances that are less accurately resolved (not shown), but fewer than 30% of the framework silicon atoms are hydroxylated. The reaction of HMS-C12 and HMS-C8 with 3-mercaptopropyltrimethoxysilane in refluxing toluene results in the silylation of 12 and 6.6% of the framework silicon sites, respectively. Clearly, the smaller pore size of HMS-C8 limits the extent of silylation. Nevertheless, the extent of silylation is substantially greater than observed for calcined MCM-41, where only 3.7% of the framework silicon atoms is functionalized in the one-step silylation process.

On the basis of the XRD patterns, N_2 adsorption isotherms, NMR spectra, and elemental analyses presented above, we may conclude that the relatively constricted channel environment for MP-HMS-C8 results in a low value for both the pore diameter (1.5 nm) and the pore volume (0.27 cm^3/g). In contrast, the retention of significant open-framework porosities for MP-HMS-C12 and MP-MCM-41 give rise to relatively large pore diameters (2.7 and 2.0 nm, respectively) and pore volumes (0.55 and 0.44 cm^3/g, respectively). Thus, HMS silicas prepared from C12 or larger amine surfactants are the most useful substrates for the design of functionalized mesoporous materials, because the neutral framework assembly ($S^\circ I^\circ$) process optimizes the surface OH group density for reaction with siloxanes. This allows for the grafting of a large number of metal-binding sites to the pore channel walls of the oxide, resulting in a highly functionalized pore wall surface. Although the surfactant is easily removed from as-synthesized HMS by solvent extraction, the complete removal of surfactant from MCM-41 prepared by electrostatic $S^+X^-I^+$ assembly requires either ion exchange under strongly acidic conditions or calcination. The calcination process depletes OH groups from the oxide surface. The grafting of siloxane to calcined MCM-41 results in an adsorbent with sparsely distributed mercaptopropyl groups in the pore channels. The pore walls of calcined MCM-41 can be rehydroxylated by acid hydrolysis and fully functionalized by reaction with a mercaptopropylsiloxane, as demonstrated by the recent work of Feng et al. (*31*). However, several acid treatment cycles are needed to form a monolayer, perhaps as many as would be required to remove the surfactant in the first place by ion exchange.

Hg(II) Adsorption on Grafted Mesostructures. In the present work, Hg(II) binding studies were carried out on siloxane-grafted mesostructures for the purpose of illustrating the importance of pore size and hydroxyl group surface density on thiol group availability for Hg(II) binding. Our earlier studies (*30*) and those of Feng et al. (*31*) have shown that the heavy metal ion selectivity is not affected by the presence of the electrolytes normally associated with groundwater and waste streams. Also, no detectable amounts of Hg(II) were adsorbed by any of the unfunctionalized mesostructures. However, as shown in Figure 4a, the binding of Hg(II) by MP-HMS-C12 and MP-HMS-C8 is quantitative up to the saturation of the binding sites at 1.5 and 0.55 mmol/g, respectively. In contrast to the quantitative Hg uptake

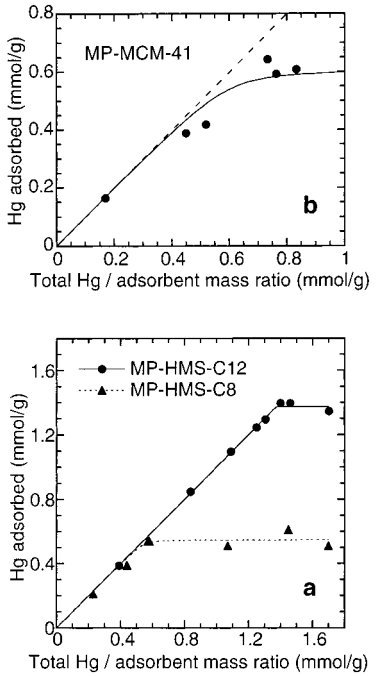

FIGURE 4. Hg(II) binding by (a) MP-HMS-C12 (solid line) and MP-HMS-C8 (dashed line), and (b) MP-MCM-41. The molar quantity of Hg(II) adsorbed per gram of adsorbent is plotted as a function of the total (initial) amount of Hg(II) per gram of adsorbent. The dashed line represents the unity slope denoting the quantitative adsorption of Hg(II).

TABLE 2. Hg(II) Adsorption Data for Mercaptopropyl-Functionalized Mesoporous Molecular Sieves

material	SH content (mmol/g)[a]	Hg(II) adsorbed (mmol/g)[b]	Hg/S molar ratio
MP-HMS-C12	1.5	1.5	1.0
MP-HMS-C8	0.90	0.55	0.61
MP-MCM-41	0.57	0.59	1.0

[a] Millimoles of S per gram of MP-functionalized adsorbent. [b] Millimoles of Hg adsorbed per gram of MP-functionalized adsorbent.

exhibited by MP-HMS-C12 and MP-HMS-C8, the adsorption of Hg(II) to MP-MCM-41 (Figure 4b) was less effective in reaching equilibrium, because Hg(II) in excess of the binding capacity is needed to achieve a saturation loading of 0.59 mmol/g.

The uptake rate of Hg(II) was noticeably slower for MP-MCM-41 than for MP-HMS. The relatively sluggish mercury absorptivity of MP-MCM-41 may be explained by the larger fundamental particle size of MCM-41 compared to HMS. HMS particles consist of loosely packed aggregates of mesoscale fundamental particles, whereas those of MCM-41 are blocky and much more monolithic. Particle size analyses of aqueous suspensions (see Supporting Information) showed that about 70% of the aggregates of HMS is smaller than 1 μm in diameter, whereas the MCM-41 aggregates are much larger (70% > 3 μm). It has been previously suggested that the larger fundamental most likely accounts for the lower catalytic activity of this mesostructure for several chemical conversions (*42*−*44*). A large particle size may also be responsible for the comparatively slower uptake of Hg(II) at sites located deep inside the adsorbent framework.

As seen from the results in Table 2, MP-HMS-C12 allows Hg(II) ions to access all of the complexing thiol groups in the material (i.e., Hg/S = 1.0). This derivative retains a large pore diameter (2.7 nm) and a significant liquid pore volume (0.55 cm^3/g), despite the high mercaptopropyl density (1.2 SH/nm^2) on the pore walls. These physical characteristics allow for the efficient binding of mercury to the mercaptopropyl groups grafted on the large, open and uniform pore channels of the adsorbent. However, in the case of the smaller pore MP-HMS-C8 system with a pore diameter of 1.5 nm and liquid pore volume of 0.27 cm^3/g, only 61% of the sites are accessible for binding (i.e., Hg/S = 0.61). Limited access to the −SH-binding sites in the smaller pore HMS derivative is consistent with the blocking of channels by the grafted ligands (*28*), particularly in the regions where the pores are constricted.

The importance of pore size on the accessibility of MP groups is supported by the observation that Hg(II) binding is quantitative for both MP-HMS-C12 and MP-MCM-41. Although MCM-41 has a comparatively small initial pore size of 2.5 nm, the pore diameter decreases by only 2.0 nm after grafting. This small decrease in pore size is attributed to the presence of fewer and more widely dispersed mercaptopropyl groups (0.57 mmol/g) on the framework pore walls (0.28 SH/nm^2) in comparison to functionalized HMS mesostructures. Consequently, pore congestion is minimized at the expense of loading capacity and the metal ions can access all of the binding sites. This interpretation is further substantiated by the retention of a significantly large pore volume in MP-MCM-41 (Table 1).

The mercaptopropylsilyl functionalized MCM-41 derivatives recently reported by Feng et al. (*31*) also are very effective heavy metal ion adsorbents, binding Hg(II) and other metal ions quantitatively to levels up to 505 mg/g. Their products, designated FMMS, have structural and reactivity features in common with MP-HMS-C12, such as the retention of framework mesoporosity and the ability to bind very high levels of Hg(II) ions to all of the thiol moieties present in the material. The preparation of FMMS derivatives from calcined MCM-41, however, requires several rehydration and mercaptopropylsiloxane treatment steps to build up a mercaptopropyl monolayer on the framework walls. This multistep process is necessary, in part, because the OH group population is substantially depleted by the surfactant calcination step. In contrast, the preparation of MP-HMS-C12 is quite facile, involving only a single mercaptopropylsilyl grafting step to afford the adsorbent. Moreover, the room-temperature synthesis used to prepare HMS and the ability to recover the surfactant by ethanol extraction offer additional processing advantages.

Compared to mesostructured metal ion adsorbents, other solid-phase complexants exhibit substantially inferior metal-binding properties. When thiol groups are grafted to the interlamellar region of clay minerals, fewer than 10% of these sites are available for metal ion binding. The low utilization of the grafted ligand sites was attributed to the "stuffing" of the interlayer region of the clay, which precluded access of the target metal ions to most of the ligand sites (*20*). Limited access was also observed for adsorbents prepared by the grafting of thiol moieties to the surface of porous silica gel. Although disordered (amorphous) silicas can exhibit surface areas and average pore diameters comparable to MCM-41 and HMS silicas, the broad pore size distributions and necking of the pores results in significant pore blockage fuctionalization. Hence, a very low availability of the thiol groups for metal binding (about 10%) is observed (*30*). The much higher metal ion loading levels observed for metal ion traps prepared from open-framework mesoporous molecular sieve silicas can be attributed to their uniquely large and relatively uniform pore structures.

Our results emphasize the advantages of molecular sieve silicas and the importance of the framework hydroxylation, nanoscale pore structure, and particle morphology in the design of efficient, high capacity heavy metal ion absorbents.

When the channel pores are comparatively narrow (diameter < 2 nm) and abundant hydroxyl sites are present, the grafting of functional units is likely to result in highly congested environments within the pore networks, drastically reducing the surface areas, pore diameters, and pore volumes. As a consequence, the effective binding of adsorbate species to these functional sites may become significantly restricted. However, framework mesostructures that possess both large pore channel dimensions (diameters > 3 nm) and abundant surface hydroxyl groups are conducive to the formation of framework channels with both a large number of functional sites and the retention of appreciable open-framework characteristics (i.e., high surface areas, pore diameters, and pore volumes). These latter features of mesoporous molecular sieve silicas, particularly as manifested in HMS materials formed by neutral surfactant assembly, should favorably impact the field of absorbent technology and the ongoing efforts to design high-performance materials for environmental cleanup and heavy metal ion recovery.

Acknowledgments

We gratefully acknowledge the U.S. National Institute of Environmental Health and Safety (Grant ES04911C), the National Science Foundation (Grant CHE-9633798), and the Natural Sciences and Engineering Research Council of Canada (Postdoctoral Fellowship to L.M.) for financial support. We also thank Professor Christian Detellier (University of Ottawa) for granting us use of the particle size analyzer.

Supporting Information Available

Particle size distribution of HMS-C12 (solid line) and MCM-41 (dashed line) (1 page). See any current masthead page for ordering information.

Literature Cited

(1) Faust, S. D.; Ali, O. M. *Chemistry of Water Treatment*; Butterworth: Boston, 1983.
(2) Huang, C. P.; Hao, O. J. *Environ. Technol. Lett.* **1989**, *10*, 863−874.
(3) Zamzow, M. J.; Eichbaum, B. R.; Sandgren, K. R.; Shanks, D. E. *Sep. Sci. Technol.* **1990**, *25*, 1555−1569.
(4) Sikalidis, C. A.; Alexiades, C.; Misaelides, P. *Toxicol. Environ. Chem.* **1989**, *20−21*, 175−180.
(5) Keizer, P.; Bruggenwert, M. G. M. *NATO ASI Ser. E* **1991**, *190*, 177−203.
(6) Leyden, D. E.; Luttrell, G. H. *Anal. Chem.* **1975**, *47*, 1612−1617.
(7) Skopenko, V. V.; Trofimchuk, A. K.; Zaitsev, V. N. *Russ. J. Inorg. Chem.* **1982**, *27*, 1458−1462.
(8) Moreira, J. C.; Gushikem, Y. *Anal. Chim. Acta* **1985**, *176*, 263−267.
(9) Gushikem, Y.; Moreira, J. C. *J. Colloid Interface Sci.* **1985**, *107*, 70−75.
(10) Howard, A. G.; Volkan, M.; Ataman, D. Y. *Analyst* **1987**, *112*, 159−162.
(11) Volkan, M.; Ataman, D. Y.; Howard, A. G. *Analyst* **1987**, *112*, 1409−1412.
(12) Iamamoto, M. S.; Gushikem, Y. *J. Colloid Interface Sci.* **1989**, *129*, 162−165.
(13) Iamamoto, M. S.; Gushikem, Y. *Analyst* **1989**, *114*, 983−985.
(14) Kubota, L. T.; Moreira, J. C.; Gushikem, Y. *Analyst* **1989**, *114*, 1385−1388.
(15) Kudryavtsev, G. V.; Miltchenko, D. V.; Yagov, V. V.; Lopatkin, A. A. *J. Colloid Interface Sci.* **1990**, *140*, 114−122.
(16) Tikhomirova, T. I.; Fadeeva, V. I.; Kudryavtsev; Nesterenko, P. N.; Ivanov, V. M.; Savitchev, A. T.; Smirnova, N. S. *Talanta* **1991**, *38*, 267−274.
(17) Andreotti, E. I. S.; Gushikem, Y. *J. Coll. Interface Sci.* **1991**, *142*, 97−102.
(18) Moreira, W. C.; Gushikem, Y.; Nascimento, O. R. *J. Colloid Interface Sci.* **1992**, *150*, 115−120.
(19) Dias Filho, N. L.; Gushikem, Y.; Rodrigues, E.; Moreira, J. C.; Polito, W. L. *J. Chem. Soc., Dalton Trans.* **1994**, 1493−1497.
(20) Mercier, L.; Detellier, C. *Environ. Sci. Technol.* **1995**, *29*, 1318−1323.
(21) Dias Filho, N. L.; Gushikem, Y.; Polito, W. L. *Anal. Chim. Acta* **1995**, *306*, 167−172.
(22) Izatt, R. M.; Bradshaw, J. S.; Bruening, R. L. *Pure Appl. Chem.* **1996**, *68*, 1237−1241.
(23) Phillips, R. J.; Fritz, J. S. *Anal. Chem.* **1978**, *50*, 1504−1508.
(24) Sugii, A.; Ogawa, N.; Hashizume, H. *Talanta* **1980**, *27*, 627−631.
(25) Deratani, A.; Sebille, B. *Anal. Chem.* **1981**, *53*, 1742−1746.
(26) Alexandratos, S. D.; Wilson, D. L. *Macromolecules* **1986**, *19*, 280−287.
(27) Tzeng, D.-L.; Shih, J.-S.; Yeh, Y.-C. *Analyst* **1987**, *112*, 1413−1416.
(28) Kantipuly, C.; Katragadda, S.; Chow, A.; Gesser, H. D. *Talanta* **1990**, *37*, 491−517.
(29) Beck, J. S.; Vartuli, J. C.; Roth, W. J.; Leonowicz, M. E.; Kresge, C. T.; Schmitt, K. D.; Chu, C. T.-W.; Olson, D. H.; Sheppard, E. W.; McCullen, S. B.; Higgins, J. B.; Schlenker, J. L. *J. Am. Chem. Soc.* **1992**, *114*, 10834−10843.
(30) Mercier, L.; Pinnavaia, T. J. *Adv. Mater.* **1997**, *9*, 500−503.
(31) Feng, X.; Fryxell, G. E.; Wang, L.-Q.; Kim, A. Y.; Liu, J.; Kemner, K. M. *Science* **1997**, *276*, 923−926.
(32) Cauvel, A.; Brunel, D.; DiRenzo, F.; Fajula, F. *AIP Conf. Proc.* **1996**, *354*, 477−484.
(33) Brunel, D.; Cauvel, A.; Fajula, F.; DiRenzo, F. *Stud. Surf. Sci. Catal.* **1995**, *97*, 173−180.
(34) Huo, Q.; Margolese, D. I.; Ciesla, U.; Feng, P.; Gier, T. E.; Sieger, P.; Leon, R.; Petroff, P. M.; Schuth, F.; Stucky, G. D. *Nature* **1994**, *368*, 317−321.
(35) Hitz, S.; Prins, R. *J. Catal.* **1997**,*168*, 194.
(36) Tanev, P. T.; Pinnavaia, T. J. *Science* **1995**, *267*, 865−867.
(37) Bagshaw, S. A.; Prouzet, E.; Pinnavaia, T. J. *Science* **1995**, *269*, 1242−1244.
(38) Marczenko, Z.; *Spectrophotometric Determination of Elements*; JohnWiley & Sons Inc.: New York, 1976.
(39) Zhang, W.; Pauly, T. R.; Pinnavaia, T. J. *Chem. Mater.* **1997**, *9*, 2491−2498.
(40) Marler, B.; Oberhagemann, U.; Vortmann, S.; Gies, H. *Micropor. Mater.* **1996**, *6*, 375.
(41) Werthmann, U.; Oberhagemann, U.; Kinski, I.; Marler, B.; Gies, H. *Proc. 2nd Euroworkshop on Zeolites*; Kaub, 1996.
(42) Zhang, W.; Froba, M.; Wang, J.; Tanev, P. T.; Wong, J.; Pinnavaia, T. J. *J. Am. Chem. Soc.* **1996**, *118*, 9164.
(43) Sayari, A. *Chem. Mater.* **1996**, *8*, 1840.
(44) Yang, R. T.; Pinnavaia, T. J.; Li, W.; Zhang, W. *J. Catal.* **1997**, *172*, 488.

Received for review July 15, 1997. Revised manuscript received May 22, 1998. Accepted June 25, 1998.

ES970622T